Kinetic Mechanism of Acetyl-CoA Synthase: Steady-State Synthesis at Variable CO/CO$_2$ Pressures

Ernest L. Maynard,[†] Christopher Sewell,[†] and Paul A. Lindahl*,[†,‡]

Contribution from the Departments of Chemistry and of Biochemistry and Biophysics, Texas A&M University, College Station, Texas 77843

Abstract: Steady-state initial rates of acetyl-CoA synthesis ($v/[\text{E}_{tot}]$) catalyzed by acetyl-CoA synthase from *Clostridium thermoaceticum* (ACS) were determined at various partial pressures of CO and CO$_2$. When [CO] was varied from 0 to 100 μM in a balance of Ar, rates increased sharply from 0.3 to 100 min^{-1}. At [CO] > 100 μM, rates declined sharply and eventually stabilized at 10 min^{-1} at 980 μM CO. Equivalent experiments carried out in CO$_2$ revealed similar inhibitory behavior and residual activity under saturating [CO]. Plots of $v/[\text{E}_{tot}]$ vs [CO$_2$] at different fixed inhibitory [CO] revealed that $V_{max}/[\text{E}_{tot}]$ (k_{cat}) decreased with increasing [CO]. Plots of $v/[\text{E}_{tot}]$ vs [CO$_2$] at different fixed noninhibitory [CO] showed that $V_{max}/[\text{E}_{tot}]$ was insensitive to changes in [CO]. Of eleven candidate mechanisms, the simplest one that fit the data best had the following key features: (a) either CO or CO$_2$ (at a designated reductant level and pH) activate the enzyme (E′ + CO $\rightleftharpoons$ E, E′ + CO$_2$/2e$^-$/2H$^+$ $\rightleftharpoons$ E); (b) CO and CO$_2$ are both substrates that compete for the same enzyme form (E + CO $\rightleftharpoons$ ECO, E + CO$_2$/2e$^-$/2H$^+$ $\rightleftharpoons$ ECO, and ECO → E + P); (c) between 3 and 5 molecules of CO bind cooperatively to an enzyme form different from that to which CO$_2$ and substrate CO bind (nCO + ECO $\rightleftharpoons$ (CO)$_n$ECO), and this inhibits catalysis; and (d) the residual activity arises from either the (CO)$_n$ECO state or a heterogeneous form of the enzyme. Implications of these results, focusing on the roles of CO and CO$_2$ in catalysis, are discussed.

Introduction

Certain archaea and bacteria employ the Wood/Ljungdahl pathway to grow chemoautotrophically on CO$_2$ and H$_2$.[1] Enzymes of the pathway reduce CO$_2$ to the methyl group of methyltetrahydrofolate (CH$_3$-THF).[2] This methyl group is first transferred to a corrinoid-iron–sulfur protein (CoFeSP) in a reaction catalyzed by methyltransferase (MeTr). Acetyl-Coenzyme A synthase (ACS; aka carbon monoxide dehydrogenase or CODH) is a bifunctional enzyme[3] that catalyzes both the reversible reduction of CO$_2$ (not bicarbonate)[4,5] to CO and the synthesis of acetyl-CoA from CO, CoA, and the CoFeSP-bound methyl group.

Acetogenic ACSs are $\alpha_2\beta_2$ tetramers containing two types of novel Ni–X–Fe$_4$S$_4$ clusters (the A- and C-clusters) and an Fe$_4$S$_4$ electron-transfer cluster (the B-cluster).[6-8] The A-cluster

is the active site for acetyl-CoA synthesis[6,7] while the C-cluster is the site of CO/CO$_2$ redox catalysis.[8,9] The enzyme is heterogeneous, in that only 30−40% of the A- and C-clusters appear to be catalytically active.[10-12]

The catalytic mechanism of acetyl-CoA synthesis is thought to involve the binding of CO to the A-cluster. An electron generated from the oxidation of CO at the C-cluster reduces the oxidized diamagnetic A-cluster (A$_{ox}$) in association with the binding of CO, yielding the $S = \frac{1}{2}$ A$_{red}$-CO state.[13] This controversial state has been implicated as both an intermediate[14,15] of acetyl-CoA synthesis and a state unable to proceed to form products.[16,17]

Methyl group transfer to ACS is possible only when an unidentified $n = 2$ redox site on ACS, known as the D-site, is reduced.[16] Barondeau and Lindahl proposed that the D-site is a disulfide/dithiol coordinated to or located near the Ni of the A-cluster, and that it facilitates nucleophilic attack of the Ni on the methyl group bound to CoFeSP. Migratory insertion of CO into the resulting CH$_3$–Ni^{2+} bond yields a Ni-acetyl group,

* To whom correspondence should be addressed at the Department of Chemistry.

† Department of Chemistry.

‡ Department of Biochemistry and Biophysics.

(1) Wood, H. G.; Ljungdahl, L. G. *Variations in Autotrophic Life*; Academic Press: London, 1991.

(2) Abbreviations: CH$_3$-THF, methyl tetrahydrofolate; CoFeSP, corrinoid iron–sulfur protein; MeTr, methyltransferase; ACS, acetyl-Coenzyme A synthase from *Clostridium thermoaceticum*, also known as CODH; CoA, coenzyme A; MV, methyl viologen; AS, ammonium sulfate; D$_{red}$, reduced state of the D-site; D$_{ox}$, oxidized state of the D-site; A$_{red}$-CO, one-electron reduced CO-bound form of the A-cluster; A$_{ox}$, the oxidized form of the A-cluster; SDS-PAGE, sodium dodecyl sulfate polyacrylamide gel electrophoresis; DTT, dithiothreitol; RDS, rate-determining step.

(3) Ragsdale, S. W.; Kumar, M. *Chem. Rev.* **1996**, *96*, 2515−2539.

(4) Bott, M.; Thauer, R. K. *Z. Naturforsch.* **1989**, *44*, 392−396.

(5) Ensign, S. A. *Biochemistry* **1995**, *34*, 5372−5381.

(6) Xia, J.; Sinclair, J. F.; Baldwin, T. O.; Lindahl, P. A. *Biochemistry* **1996**, *35*, 1965−1971.

(7) Xia, J.; Hu, Z.; Popescu, C. V.; Lindahl, P. A.; Münck, E. *J. Am. Chem. Soc.* **1997**, *119*, 8301−8312.

(8) Hu, Z. G.; Spangler, N. J.; Anderson, M. E.; Xia, J. Q.; Ludden, P. W.; Lindahl, P. A.; Münck, E. *J. Am. Chem. Soc.* **1996**, *118*, 830−845.

(9) Anderson, M. E.; Lindahl, P. A. *Biochemistry* **1994**, *33*, 8702−8711.

(10) Shin, W.; Anderson, M. E.; Lindahl, P. A. *J. Am. Chem. Soc.* **1993**, *115*, 5522−5526.

(11) Shin, W.; Lindahl, P. A. *J. Am. Chem. Soc.* **1992**, *114*, 9718−9719.

(12) Fraser, D. M.; Lindahl, P. A. *Biochemistry* **1999**, *38*, 15697−15705.

(13) Ragsdale, S. W.; Ljungdahl, L. G.; DerVartanian, D. V. *Biochem. Biophys. Res. Commun.* **1982**, *108*, 658−663.

(14) Gorst, C. M.; Ragsdale, S. W. *J. Biol. Chem.* **1991**, *266*, 20687−20693.

(15) Menon, S.; Ragsdale, S. W. *Biochemistry* **1996**, *35*, 12119−12125.

(16) Barondeau, D. P.; Lindahl, P. A. *J. Am. Chem. Soc.* **1997**, *119*, 3959−3970.

(17) Grahame, D. A.; Khangulov, S.; Demoll, E. *Biochemistry* **1996**, *35*, 593−600.

subsequent nucleophilic attack of which by CoA yields acetyl-CoA and the rereduced D-site.[16,18]

We recently examined the effect of CO_2 on the catalytic synthesis of acetyl-CoA, and discovered that it is a substrate for this activity.[19] This implies that CO_2 is reduced to CO at the C-cluster and that CO migrates to the A-cluster for use in acetyl-CoA synthesis. We also found that CO is not released into solution for this migration, but travels through a protein-encapsulated tunnel from the C- to the A-cluster. Since these clusters are located in separate subunits and show no magnetic interactions when both are in $S = {}^1\!/_2$ paramagnetic states, the tunnel may be >10 Å long. A subsequent study by Ragsdale and co-workers provided further evidence for this tunnel.[20] Molecular tunnels connect active sites in other multifunctional enzymes.[21−23]

Since CO is known to react with the C-cluster and the A-cluster, there must be at least 2 CO-binding sites on the enzyme. However, additional sites have been proposed.[9,24−28] Anderson and Lindahl suggested that CO or CO_2 (in the presence of a reductant) reactivate cyanide-inhibited enzyme by binding to a "modulator" site.[9] Seravalli et al. suggested that two CO molecules bind to the C-cluster.[25] Russell and Lindahl interpreted their CO/CO_2 potentiometric titrations in terms of a redox-cooperativity in the presence of CO_2.[26] Ludden and co-workers have recently reported that CODH from *Rhodospirillum rubrum* is activated upon binding a CO molecule at the C-cluster.[24] CO has also been found to partially inhibit the ACS-catalyzed exchange of free CoA with acetyl-CoA.[29,30]

These studies suggest that the effects of CO and CO_2 with ACS are complicated, possibly involving multiple roles. Moreover, the discovery that both CO_2 and CO are substrates for the synthesis of acetyl-CoA raises issues regarding the kinetic mechanism. CO_2 behaves as a classical Michaelis−Menten substrate ($K_m = 320 \pm 50$ μM; $k_{cat}/K_m = 0.53 \pm 0.07$ μM^{-1} min^{-1}),[19] while analogous kinetic parameters for CO have not been reported. Also unknown are whether CO and CO_2 are competitive substrates and whether their catalytic properties are additive. To address these issues, we measured steady-state acetyl-CoA synthase activity at various concentrations of CO and CO_2, and fit kinetic models to the data. In this paper, these experiments are described, a kinetic mechanism emphasizing the roles of CO and CO_2 in catalysis is proposed, and implications are discussed.

Experimental Procedures

ACS Purification. *Clostridium thermoaceticum* cells were grown and harvested as described.[31,32] Protein purification was performed in a Vacuum/Atmospheres HE-453 glovebox containing <1 ppm O_2, as

monitored continuously (Teledyne model 310 analyzer). ACS was purified from cell paste, using a modified procedure (10 mM DTT was included in all buffers).[33] ACS was 90−94% pure, as quantified by imaging Coomassie Blue (Bio-Rad) stained SDS-PAGE gels with an AlphaImager 2000 (Alpha Innotech Corp.) densitometer. ACS catalyzed CO oxidation[33] and acetyl-CoA synthesis (assayed as described below with 1 atm CO_2) with specific activities of 350 and 1.3 μmol min^{-1} mg^{-1}, respectively. Protein concentrations were determined by the Biuret method.[34] ACS, CoFeSP, and MeTr have molecular masses of 154 700 Da /$\alpha\beta$,[35] 89 000 Da /$\alpha\beta$,[36] and 57 280 Da/α_2,[37] respectively.

Buffer A (50 mM MES pH 6.3) was rendered CO_2-free as follows. MES (Sigma) was dissolved in distilled−deionized water to a final concentration of 50 mM, pH 3.3, filtered, degassed using an anaerobic Schlenk line, and brought into the box. The pH was adjusted to 6.30 by using anaerobically prepared 50% (w/v) KOH. Buffer A was sparged with O_2-scrubbed (Oxisorb, MG Industries) Ar for 30 min prior to use. ACS activity assays were used to detect residual CO_2 dissolved in Buffer A. Without added CO or CO_2, ACS catalyzed the synthesis of acetyl-CoA at an initial rate of 0.1 μM min^{-1}, corresponding to 0.6 μM CO_2 in solution.

Dithionite-reduced ACS was thawed, concentrated using a Centricon-100 (Amicon), and chromatographed using a Sephadex G-25 column (1 cm × 20 cm) equilibrated with Buffer A containing 1.0 mM DTT. Dithionite-free enzyme was eluted at 0.5 mL/min. Samples were divided into aliquots and simultaneously frozen in liquid N_2.

CoFeSP Purification. Rust-brown colored fractions eluting prior to ACS on DEAE Sephacel (Pharmacia) were concentrated by ultrafiltration through a YM30 membrane (Amicon), made 10% in ammonium sulfate (AS), and applied to a phenyl Sepharose (Pharmacia) column (5 cm × 17 cm) equilibrated in Buffer B (50 mM Tris-Cl, pH 8.0, 2.0 mM dithionite, 10 mM DTT) plus 10% AS.[16] The column was washed with 500 mL of Buffer B plus 10% AS, and proteins were eluted with a linear gradient containing 10−2.5% AS (750 mL of each). Rust-brown fractions were combined, concentrated, diluted with 5 volumes of Buffer B, and loaded onto a DEAE Sephacel column (5 cm × 16 cm) equilibrated with Buffer B. The column was washed with 800 mL of Buffer B containing 0.1 M NaCl. CoFeSP eluted with a linear gradient containing 0.1−0.4 M NaCl (500 mL of each). Combined CoFeSP fractions were removed from the box and frozen in liquid N_2. Active fractions were 92−95% pure according to SDS-PAGE analysis. CoFeSP was assayed (as described below with 1 atm of CO_2) for its ability to assist in catalyzing the synthesis of acetyl-CoA, by varying its concentration at fixed [ACS] (2 μM) and [MeTr] (10 μM). Within the range tested (0 − 8 μM CoFeSP) the rate of acetyl-CoA synthesis was linear, with a specific activity of 0.10 μmol min^{-1} mg^{-1}.

Dithionite-reduced CoFeSP was thawed, concentrated using a Centricon-30, and chromatographed using Sephadex G-25 (1 cm × 20 cm) equilibrated in Buffer A. CoFeSP was collected into a 1-cm quartz cuvette and scanned from 350−620 nm (Spectral Instruments model SI 440). Residual dithionite was reacted with thionin (Aldrich) (2.5 mM, in Buffer A) until the absorbance at 604 nm, due to unreacted thionin, increased.[16] The sample was concentrated and excess thionin was removed by G-25 chromatography, as above. Dithionite-free thionin-oxidized CoFeSP was concentrated, divided into aliquots, and frozen as above.

MeTr Purification. MeTr assay solution contained the following (final concentrations): Buffer C (50 mM Na-phosphates, pH 6.3, 1.0

(18) Ragsdale, S. W.; Wood, H. G. *J. Biol. Chem.* **1985**, *260*, 3970−3977.

(19) Maynard, E. L.; Lindahl, P. A. *J. Am. Chem. Soc.* **1999**, *121*, 9221−9222.

(20) Seravalli, J.; Ragsdale, S. W. *Biochemistry* **2000**, *39*, 1274−1277.

(21) Thoden, J. B.; Holden, H. M.; Wesenberg, G.; Raushel, F. M.; Rayment, I. *Biochemistry* **1997**, *36*, 6305−6316.

(22) Hyde, C. C.; Ahmed, S. A.; Padlan, E. A.; Miles, E. W.; Davies, D. R. *J. Biol. Chem.* **1988**, *263*, 17857−17871.

(23) Krahn, J. M.; Kim, J. H.; Burns, M. R.; Parry, R. J.; Zalkin, H.; Smith, J. L. *Biochemistry* **1997**, *36*, 11061−11068.

(24) Heo, J.; Staples, C. R.; Halbleib, C. M.; Ludden, P. W. *Biochemistry* **2000**, *39*, 7956−7963.

(25) Seravalli, J.; Kumar, M.; Lu, W.-P.; Ragsdale, S. W. *Biochemistry* **1997**, *36*, 11241−11251.

(26) Russell, W. K.; Lindahl, P. A. *Biochemistry* **1998**, *37*, 10016−10026.

(27) Ensign, S. A.; Hyman, M. R.; Ludden, P. W. *Biochemistry* **1989**, *28*, 4973−4979.

(28) Hyman, M. R.; Ensign, S. A.; Arp, D. J.; Ludden, P. W. *Biochemistry* **1989**, *28*, 6821−6826.

(29) Lu, W.; Ragsdale, S. W. *J. Biol. Chem.* **1991**, *266*, 3554−3564.

(30) Pezacka, E.; Wood, H. G. *J. Biol. Chem.* **1986**, *261*, 1609−1615.

(31) Lundie, L. L., Jr.; Drake, H. L. *J. Bacteriol.* **1984**, *159*, 700−703.

(32) Loke, H.-K.; Bennett, G. N.; Lindahl, P. A. *Proc. Natl. Acad. Sci. U.S.A.* **2000**, *97*, 12530−12535.

(33) Shin, W.; Lindahl, P. A. *Biochim. Biophys. Acta* **1993**, *1161*, 317−322.

(34) Pelley, J. W.; Garner, C. W.; Little, G. H. *Anal. Biochem.* **1978**, *86*, 341−343.

(35) Morton, T. A.; Rundquist, A. R.; Ragsdale, S. W.; Shanmugasundaram, T.; Wood, H. G.; Ljundahl, L. G. *J. Biol. Chem.* **1991**, *266*, 23824−23828.

(36) Lu, W. P.; Schiau, I.; Cunningham, J. R.; Ragsdale, S. W. *J. Biol. Chem.* **1993**, *268*, 5605−5614.

(37) Roberts, D. L.; Zhao, S. Y.; Doukov, T.; Ragsdale, S. W. *J. Bacteriol.* **1994**, *176*, 6127−6130.

mM DTT), 50 μM $\alpha\beta$ CoFeSP, 1.0 mM CH$_3$-THF (Sigma, disodium salt), and 500 μM Ti(III) citrate prepared[38] from Ti(III) chloride (Aldrich) at 30 $\pm$ 2 °C. To 0.50 mL of assay solution in a 0.5 cm quartz cuvette was added 50$-$ 100 μL of solution containing MeTr. [Co^{1+}FeSP] (calculated using $\Delta\epsilon_{390\ nm} = 7.9$ mM^{-1} cm^{-1}, experimentally determined) was monitored vs time.

Active fractions, which eluted after ACS on the DEAE Sephacel column (from the ACS prep), were concentrated by ultrafiltration using a YM30 membrane, diluted with 2 volumes of Buffer C, and applied to a DEAE Biogel-A (Bio-Rad) column (5 cm × 12.7 cm) equilibrated in Buffer C. The column was washed with 700 mL of Buffer C containing 0.15 M NaCl. Proteins were eluted with a linear gradient containing 0.15$-$0.4 M NaCl (600 mL of each). Active fractions were concentrated, diluted with 5 volumes of Buffer D (50 mM Tris-Cl, pH 7.6, 1.0 mM DTT), made 6.0% in AS, and applied to a phenyl Sepharose column (5 cm × 14 cm) equilibrated in Buffer D containing 6.0% AS. The column was washed with 1 L of Buffer D containing 6.0% AS. Proteins were eluted with a linear gradient containing 6.0$-$0% AS in Buffer D (600 mL of each). Active fractions were combined, concentrated, and immediately frozen in liquid N$_2$. MeTr was >95% pure according to SDS-PAGE analysis and had a specific activity of 5.0 μmol min^{-1} mg^{-1}. Purified MeTr was thawed, concentrated using a Centricon-10 (Amicon), diluted with 25 volumes of Buffer A containing 1.0 mM DTT, and reconcentrated. After repeating this procedure 5×, aliquots were frozen as above.

Acetyl-CoA Synthase Assay. CH$_3$-THF and Coenzyme A (Sigma, sodium salt) were dissolved in Buffer A to give 63.5 $\pm$ 0.2 and 34.5 $\pm$ 0.3 mM stock solutions, respectively. Concentrations were determined using $\epsilon_{290} = 30.8$ mM^{-1} cm^{-1} for CH$_3$-THF[39,40] and $\epsilon_{260} = 16.8$ mM^{-1} cm^{-1} for CoA.[41] DTT was added (1.0 mM final) to the CoA solution to prevent oxidation. Each solution was divided into aliquots and frozen as above.

Various amounts of CO (MG Industries, research grade), CO$_2$ (MG Industries, anaerobic grade), and Ar were mixed with a flowmeter (MG Industries, series 7941-AS2 4-tube) and passed into a reaction vessel.[19] The flowmeter was calibrated by measuring in triplicate the rate of water displaced from a volumetric flask. Henry's law constants for CO and CO$_2$ at 30 °C are 0.98 mM/atm[41] and 31 mM/atm,[42] respectively.

Methyl viologen (Sigma; MV$^{2+/1+}$; $E^{o\prime} = -0.44$ V vs NHE[43]) was enzymatically reduced,[19] standardized by titration against K$_3$Fe(CN)$_6$, and used immediately (average of 12 measurements yielded 68 $\pm$ 2% reduction). To a 5.0 mL conical vial were added, in the following order, Buffer A, CH$_3$-THF (2.0 mM), CoFeSP (30 μM), MeTr (10 μM), and MV^{1+} (1.0 mM), yielding 0.50 mL total volume (final concentrations). The assay solution was mixed and then transferred into a reaction vessel. The vessel was sealed, removed from the glovebox, flushed with 15$-$20 volumes of the desired mixture of gases, and returned to the box. For experiments involving varied [CO$_2$], CO$_2$ was injected by syringe (Hamilton Gastight). The reaction mixture was incubated 15 min at 30 $\pm$ 2 °C in dim light. Acetyl-CoA synthesis was initiated by syringe injection of a CoA/ACS solution affording 1.0 mM CoA, 0.3 μM $\alpha\beta$ ACS, and 50 μM DTT (final concentrations). Aliquots (80 μL) were removed by syringe at various times and analyzed for acetyl-CoA by reversed phase HPLC.[19] Initial rates were determined by linear least-squares regression analysis of [acetyl-CoA] vs time plots. Ninety-seven data points (rates at various [CO] and [CO$_2$]) were analyzed.

Conditions Employed in Assays. A reductant was required when CO$_2$ was used as the substrate. Although the resulting solution potential was sufficient to yield only ~20% of the theoretical V_{max}/[E$_{tot}$],[19] MV^{1+} was chosen because of its stability at the experimental pH. Our analysis assumes that the steady-state ratios of [MV^{1+}]/[MV^{2+}] and [D$_{red}$]/D$_{ox}$] were the same under all conditions employed (i.e. independent of [CO]

and [CO$_2$]). This assumption should be valid, as the initial [MV^{1+}]/[MV^{2+}] ratio of the stock solution (2.1 $\pm$ 0.2) was nearly the same for each experiment, and all steps performed after introducing this reductant were strictly anaerobic. Because [MV] and [H$^+$] were constant, the "CO$_2$" included in our mechanisms (and conclusions) should be viewed as an undifferentiated species CO$_2$/2e$^-$/2H$^+$ rather than a CO$_2$ molecule.

The initial CH$_3$-THF concentration was 200 times its K_m of 10 μM,[44] and the amount consumed during reaction (~0.3 mM) was insignificant. The high concentrations of CH$_3$-THF and MeTr ensured that methyl group transfer to CoFeSP did not affect the rate of acetyl-CoA synthesis within the conditions employed. These high concentrations also ensured that the concentration of substrate CH$_3$-Co^{3+}FeSP would remain constant and high, and that the concentration of product Co^{1+}FeSP would remain constant and low, relative to [ACS]. The large volume of the reaction vessels (~270 mL) ensured that [CO] and [CO$_2$] did not change significantly during reaction. The initial [CoA] was substantially greater than its K_d of 10 μM[45] and its K_m of 50 μM for the CO/Acetyl-CoA exchange reaction.[46] Thus, under the conditions employed, only changes in [CO] and [CO$_2$] affected the initial rate of reaction.

Modeling and Simulations. Eleven kinetic mechanisms were analyzed, designated U1AT, U2AT, U3AT, U4AT, U5AT, U6AT, C4AT, M4AT, R4AT, U4AO, and U4NT.[47] These included a "residual" activity at high inhibitor concentrations that arose either from a partially active inhibited enzyme form (U4AO) or from a distinct enzyme form not inhibited by CO (all other models). Each mechanism involved N enzyme forms. Differential equations describing the time-dependent concentrations of $N - 1$ of these forms were set equal to 0 in accordance with the steady-state approximation. Resulting equations and the conservation relationship [E$_{tot}$] $= \sum_{i=1}^{N}$[E$_i$] were solved using Maple version 6.0 (Waterloo Maple, Inc.), for [E] and [E$_{res}$] (the enzyme form that gives rise to the residual activity) as a function of [CO], [CO$_2$], and [E$_{tot}$]. These expressions were substituted into the rate expression d[P]/d$t = v = k_p$[E] $+ k_{res}$[E$_{res}$], where k_p and k_{res} are turnover numbers for the major and residual enzyme forms. The expression for maximal rate $V_{max} = k_{cat}$[E$_{tot}$] was determined by setting each substrate concentration to ∞ and all inhibitor concentrations to 0. The expression for the K_m of a given substrate was obtained by setting the other substrate and inhibitor concentrations to 0 and solving for the substrate concentration when $v = {}^1/_2V_{max}$. Expressions describing k_{cat}/K_m and K_m in terms of microscopic rate constants were substituted into the equation $v = k_p$[E] $+ k_{res}$[E$_{res}$] as a means of minimizing the number of unknowns.

Resulting steady-state velocity equations were fit to 14 data sets (plots of $(v/$[E$_{tot}$])$_{dat}$ vs either increasing [CO]$_{dat}$ at fixed [CO$_2$]$_{dat}$ or increasing [CO$_2$]$_{dat}$ at fixed [CO]$_{dat}$) using a computer program written in C. The Adaptive Simulated Annealing (ASA) algorithm[48] was used to search for best-fit values of the parameters for each equation. A cost function returned the sum of the squares of the residuals between the data points and the graph of the equation evaluated at the current parameter values. ASA was used to find parameter values that minimized this difference. Relative errors for each model are reported in Table 1. ASA was also used to determine the uncertainty in each parameter by separately finding the value that would make the cost 1.5 times its minimal value, fixing all other parameters at best-fit values. Simulations of each data set (i.e. v_{sim}/[E$_{tot}$] vs either [CO]$_{sim}$ at fixed [CO$_2$]$_{sim}$ or [CO$_2$]$_{sim}$ at fixed [CO]$_{sim}$) consisted of 1000 simulation points spanning the same range as the data.

(38) Seefeldt, L. C.; Ensign, S. A. *Anal. Biochem.* **1994**, *221*, 379$-$386.
(39) Blair, J. A.; Saunders: K. J. *Anal. Biochem.* **1970**, *34*, 376$-$381.
(40) Gupta, V. S.; Huennekens, F. M. *Arch. Biochem. Biophys.* **1967**, *120*, 712$-$718.
(41) Budavari, S. *The Merck Index*, 11 ed.; Merck & CO., Inc.: Rahway, NJ, 1989.
(42) Butler, J. N. *Carbon Dioxide Equilibria and Their Applications*; Addison-Wesley: Reading, MA, 1982.
(43) Michaelis, L.; Hill, E. S. *J. Am. Chem. Soc.* **1933**, *55*, 1481.

(44) Zhao, S. Y.; Roberts, D. L.; Ragsdale, S. W. *Biochemistry* **1995**, *34*, 15075$-$15083.
(45) Wilson, B. E.; Lindahl, P. A. *J. Biol. Inorg. Chem.* **1999**, *4*, 742$-$748.
(46) Ramer, S. E.; Raybuck, S. A.; Orme-Johnson, W. H.; Walsh, C. T. *Biochemistry* **1989**, *28*, 4675$-$4680.
(47) Mechanisms were distinguished by a four-alphanumeric code. The first alphanumeric (U, C, M, or R) indicates Uncompetitive, Competitive, Mixed, or Reductive inhibition. The second (1$-$6) indicates the number of CO's presumed to inhibit activity. The third alphanumeric (A or N) indicates whether CO/CO$_2$ Activation was assumed or Not assumed. The fourth alphanumeric (O or T) indicates whether one or two terms are present in the rate equation.
(48) Ingber, L. *Math. Comput. Modeling* **1989**, *12*, 967$-$973.

Table 1

| mechanism	description	unknowns	rel error
U1AT	<u>U</u>ncompetitive; **<u>1</u>** CO's bind ECO; <u>A</u>ctivation; <u>T</u>wo terms	10	5.4
U2AT	<u>U</u>ncompetitive; **<u>2</u>** CO's bind ECO; <u>A</u>ctivation; <u>T</u>wo terms	11	1.8
U3AT	<u>U</u>ncompetitive; **<u>3</u>** CO's bind ECO; <u>A</u>ctivation; <u>T</u>wo terms	12	1.1
U4AT	<u>U</u>ncompetitive; **<u>4</u>** CO's bind ECO; <u>A</u>ctivation; <u>T</u>wo terms	13	1.0
U5AT	<u>U</u>ncompetitive; **<u>5</u>** CO's bind ECO; <u>A</u>ctivation; <u>T</u>wo terms	14	0.98
U6AT	<u>U</u>ncompetitive; **<u>6</u>** CO's bind ECO; <u>A</u>ctivation; <u>T</u>wo terms	15	0.96
C4AT	<u>C</u>ompetitive; **<u>4</u>** CO's bind ECO; <u>A</u>ctivation; <u>T</u>wo terms	13	4.6
M4AT	<u>M</u>ixed; **<u>4</u>** CO's bind ECO; <u>A</u>ctivation; <u>T</u>wo terms	17	1.0
R4AT	**<u>1</u>** CO <u>R</u>educes and **<u>3</u>** CO's bind ECO; <u>A</u>ctivation; <u>T</u>wo terms	13	5.9
U4NT	<u>U</u>ncompetitive; **<u>4</u>** CO's bind ECO; <u>N</u>o activation; <u>T</u>wo terms	10	2.2
U4AO	<u>U</u>ncompetitive; **<u>4</u>** CO's bind ECO; <u>A</u>ctivation; <u>O</u>ne term	12	1.1
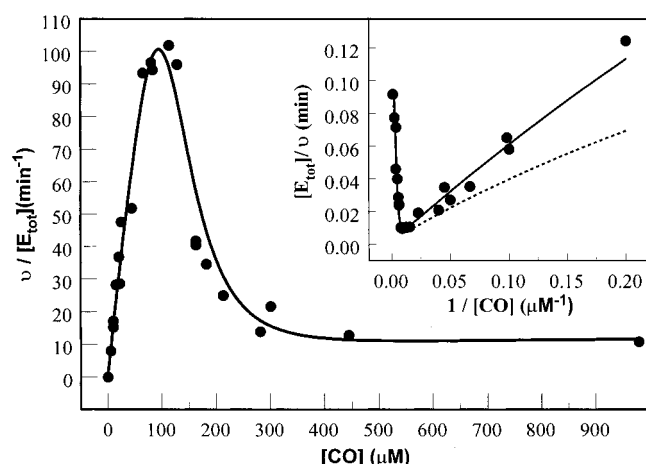
Figure 1. Initial rate of acetyl-CoA synthesis at increasing [CO] under an Ar atmosphere. Data (●) were obtained as described in the Experimental Procedures. The solid line is the best-fit simulation generated by using eq 1 (model U4AT, Table 1) and the best-fit parameters (see text). Inset: Double reciprocal plot of data (●), best fit (—), and fit without activation (mechanism U4NT) by CO/CO_2 (- - -).

Figure 2. Initial rate of acetyl-CoA synthesis at increasing [CO] under 3.8 (●) and 1.0 mM (■) [CO_2]. Other conditions were as in Figure 1. Inset: Double reciprocal plot and comparison with data of Figure 1 (▼).

Results

Assay Conditions. The catalytic synthesis of acetyl-CoA by ACS is exceedingly complex, involving three proteins (ACS, CoFeSP, and MeTr), seven components (CO, CO_2, CH_3-THF, CoA, MV^{1+}, MV^{2+}, and H^+), and the strict exclusion of O_2. In the past, this complexity has made detailed kinetic studies difficult. We have succeeded in performing such experiments by controlling and fixing numerous variables and focusing on the effects of CO and CO_2. As a result, the kinetic parameters reported here are *apparent* rather than true values, applicable only under the conditions employed. Refer to Experimental Procedures for details.

CO Activation of ACS. To determine the steady-state kinetic parameters for CO, initial steady-state rates of acetyl-CoA synthesis, normalized to the total enzyme concentration (v/[E_{tot}]), were measured as the concentration of CO was varied in a balance of Ar (Figure 1, solid circles). As [CO] increased from 0 to 100 μM, v/[E_{tot}] increased from 0.3 to 100 min^{-1}. When plotted in double-reciprocal form (Figure 1, inset), the data in this range yielded a straight line, suggesting a hyperbolic dependence of rate on [CO], as expected for a Michaelis–Menten substrate. However, the slope of this line is far steeper than would be observed for a standard substrate. As we show below, the only models able to simulate this slope (and the observed maximal activity) assume that the binding of CO to ACS, or the reduction of some site on ACS caused by the binding and subsequent oxidation of CO to CO_2, activates ACS for catalysis. The unbound or oxidized form of ACS is either
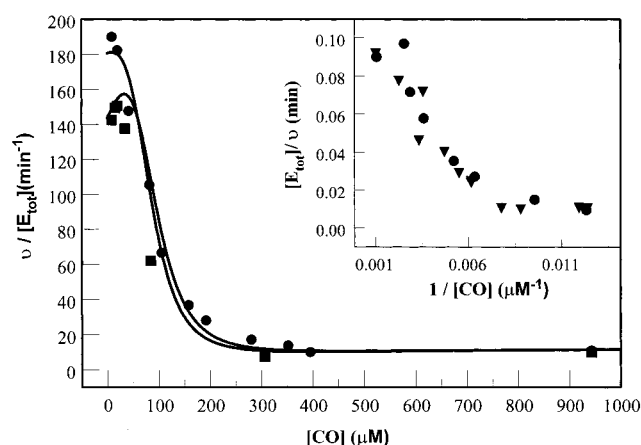
inactive or less active than the CO-bound or CO-reduced form. Thus, CO is both an activator and a substrate of ACS-catalyzed acetyl-CoA synthesis.

CO Inhibition of ACS and the Residual Activity. As [CO] increased above 100 μM, rates declined sharply. By 300 μM CO, the rate was 20 min^{-1}, 20% of maximal. This reveals that, in addition to being a substrate and an activator, CO inhibits ACS from catalyzing acetyl-CoA synthesis. The rate of catalysis continued to decline as [CO] increased, eventually stabilizing at a residual rate of 10 min^{-1} under an atmosphere of CO (980 μM). This rate is similar to those reported previously under saturating CO conditions,[49] including 7,[50] 15,[51] and 20 min^{-1}.[52]

Equivalent data obtained with 3.8 mM CO_2 (Figure 2, solid circles) showed a maximal rate of nearly 200 min^{-1} at 10 μM [CO]. At higher [CO], rates again declined and eventually stabilized at 10 min^{-1}. These data demonstrate that CO also inhibits catalysis in the presence of CO_2. Similar data were obtained with 1.0 mM CO_2 (Figure 2, solid squares), except that the maximal rate was somewhat less (150 min^{-1}). Given the previously determined K_m value for CO_2 (320 μM),[19] this difference in maximal rates probably reflects incomplete saturation of ACS. For both CO_2 concentrations used, residual rates were similar to that obtained under Ar. A double-reciprocal plot

(49) The latter two rates were obtained by dividing the published rates (obtained at 55 °C) by 8 to account for the temperature difference. Rates were not corrected for the lower solubility of CO in solution at 55 °C. This solubility difference may account for the ∼2-fold faster rates of catalysis obtained.

(50) Lu, W.; Harder, S. R.; Ragsdale, S. W. *J. Biol. Chem.* **1990**, *265*, 3124−3133.

(51) Roberts, J. R.; Lu, W.-P.; Ragsdale, S. W. *J. Bacteriol.* **1992**, *174*, 4667−4676.

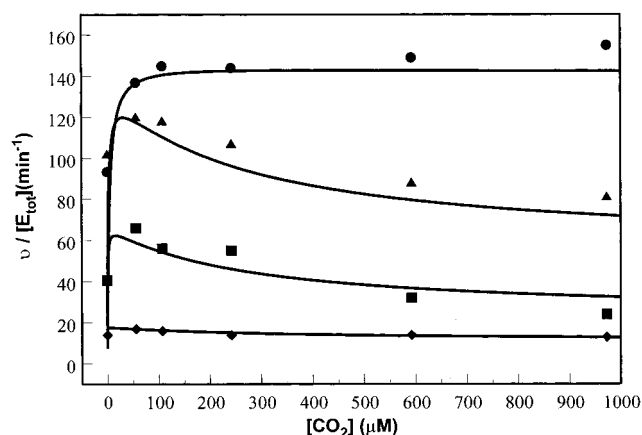(52) Menon, S.; Ragsdale, S. W. *Biochemistry* **1998**, *37*, 5689−5698.

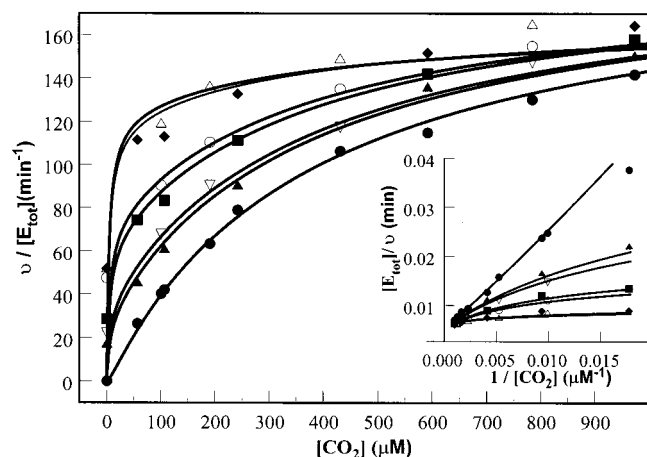**Figure 3.** Initial rate of acetyl-CoA synthesis at increasing $[CO_2]$ and 66 (●), 114 (▲), 163 (■), and 282 μM (♦) [CO].

Figure 4. Initial rate of acetyl-CoA synthesis at increasing $[CO_2]$ and 0 (●), 10 (▲), 12 (▽), 22 (■), 25 (○), 44 (♦), and 46 μM (△) [CO]. Inset: Double reciprocal plot.

of the inhibitory region (Figure 2, inset) indicates a similar [CO]-dependence for titrations performed in CO_2 and Ar.

CO Functional Regions. CO is an activator, as well as a substrate for catalysis. At high concentrations, CO partially inhibits catalysis, as evidenced by the residual activity. These functions operate throughout the [CO] range employed in these experiments, but certain functions dominate within a given concentration "region". Despite an overlap of functions, 0–20 μM CO will be called the *Activation* region, 20–100 μM will be called the *Substrate* region, 100–300 μM will be called the *Inhibitory* region, and 300–980 μM will be called the *Residual* region.

Relationship of CO and CO_2 in the Inhibitory Region. We wanted to determine whether CO inhibited catalysis by a competitive or uncompetitive mechanism, or by a mixture of the two (mixed inhibition). These mechanisms were distinguished graphically, by plotting rates as a function of $[CO_2]$ at different fixed [CO] in the *Inhibitory* region. The resulting plots (Figure 3) did not coalesce toward a single $v/[E_{tot}]$ value (i.e. k_{cat}) as $[CO_2]$ increased (which would have indicated competitive inhibition). Rather, $v/[E_{tot}]$ decreased with increasing [CO], consistent with uncompetitive inhibition.

Probing the Substrate/Activation Region. The rate of catalysis was measured as a function of $[CO_2]$ at different [CO] in the *Substrate/Activation* region to determine whether substrate CO and CO_2 competed for the same enzyme form. The resulting direct plots (Figure 4) approached the same $v/[E_{tot}]$ as $[CO_2]$
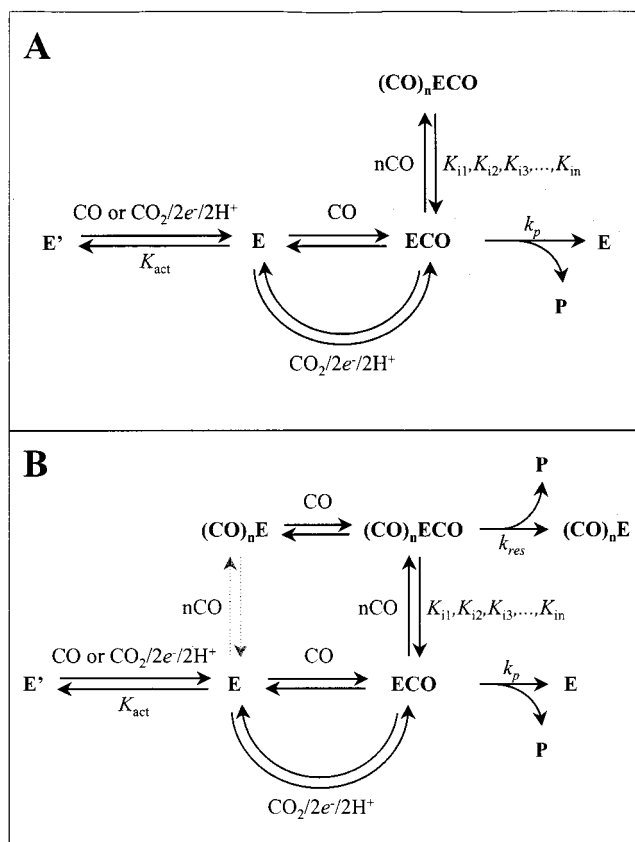

Figure 5. (A) Kinetic mechanism of the "major" activity from U4AT. (B) Mechanism U4AO. See text for details.

increased, and the corresponding double-reciprocal plots (Figure 4, inset) coalesced toward a single $[E_{tot}]/v$ value. This type of pattern is consistent with a competitive mode of interaction and indicates that CO and CO_2 compete for the same enzyme form during the catalytic synthesis of acetyl-CoA. Plots of $[E_{tot}]/v$ vs $1/[CO_2]$ at nonzero [CO] revealed nonlinear behavior (Figure 4, inset). This can be attributed to CO's ability to serve as a substrate in catalysis.

Data Analysis. Eleven kinetic mechanisms were evaluated for their ability to simulate the data (as determined by the relative errors in Table 1), and to do so with the fewest unknown parameters. Using these criteria, the best mechanism, called U4AT[47] and illustrated in Figure 5A, is described by the steady-state rate equation

$$\frac{v}{[E_{tot}]} = \frac{\left(\frac{k_{cat}}{K_m}\right)_{CO}[CO] + \left(\frac{k_{cat}}{K_m}\right)_{CO_2}[CO_2]}{T\frac{[CO]}{K_{m,CO}} + T\frac{[CO_2]}{K_{m,CO_2}} + A} + \frac{k_{res}[CO]}{K_{m,res} + [CO]} \quad (1)$$

where

$$T = 1 + \sum_{j=1}^{n}\left(\frac{[CO]^j}{\prod_{k=1}^{j}K_{ik}}\right) \quad (2)$$

and

$$A = 1 + \frac{K_{act}(k_{a1} + k_{a3})}{k_{a1}[CO] + k_{a3}[CO_2]} \quad (3)$$

The first term of U4AT describes the "major" activity that dominates in the *Activation*, *Substrate*, and *Inhibitor* regions. The second term represents the residual activity evident in the *Residual* region. In this mechanism, the residual activity arises from a second enzyme form which utilizes CO as a classical Michaelis−Menten substrate. At infinite [CO], only the first term approaches zero. According to U4AT, enzyme in the inactivated form E′ reacts with either CO or CO_2, yielding activated form E. In the next step, CO and CO_2 compete for E, yielding CO bound form ECO. ECO reacts with CH_3-Co^{3+}-FeSP and CoA (represented as a single step) yielding product (acetyl-CoA) and E. Four CO molecules bind sequentially to ECO, yielding unproductive $(CO)_n$ECO ($n = 1-4$) forms of the enzyme. Thus, U4AT assumes that 4 CO molecules inhibit the synthesis of acetyl-CoA uncompetitively with respect to "substrate" CO and CO_2. The solid lines in Figures 1−4 represent the best-fit simulation obtained using U4AT. Best-fit kinetic parameters for CO and CO_2, obtained at 30 °C, were as follows: $k_{cat,CO} = 900 \pm 300$ min^{-1}, $K_{m,CO} = 300 \pm 100$ μM, $(k_{cat}/K_m)_{CO} = 3.2 \pm 0.4$ μM^{-1} min^{-1}, $k_{cat,CO_2} = 200 \pm 30$ min^{-1}, $K_{m,CO_2} = 380 \pm 40$ μM, $(k_{cat}/K_m)_{CO_2} = 0.52 \pm 0.04$ μM^{-1} min^{-1}, $K_{act} = 6 \pm 3$ μM, $k_{a1} = 10 \pm 8$ μM^{-1} min^{-1}, $k_{a3} = 6000 \pm 3000$ μM^{-1} min^{-1}, $k_{res} = 10 \pm 5$ min^{-1}, and $K_{m,res} = 200 \pm 100$ μM. The best-fit inhibition constants were $K_{i1} = 900 \pm 300$ μM, $K_{i2} = 50 \pm 10$ μM, $K_{i3} = 40 \pm 10$ μM, $K_{i4} = 50 \pm 30$ μM.[53]

U4AT fits the data with high fidelity. The lower values of the last three inhibition constants (K_{i2}, K_{i3}, and K_{i4}) relative to K_{i1} indicate positive-cooperative binding and inhibition of the enzyme by CO. The (k_{cat}/K_m) values reflect the efficiency by which CO or CO_2 form ECO. The best-fit $(k_{cat}/K_m)_{CO}$ is 6 times greater than that of CO_2, suggesting that CO is a better substrate than CO_2. However, given that these values are apparent (see Experimental Procedures), this difference may simply reflect the sub-optimal reducing conditions used. Using CO_2 as a substrate, we have studied the dependence of solution redox potential on initial velocity and found that under maximally reducing conditions, k_{cat,CO_2} was enhanced by a factor of 4.6.[19] Everything else being equal, correcting the best-fit k_{cat} for this factor would increase $(k_{cat}/K_m)_{CO_2}$ to a value (namely 2.4 μM^{-1} min^{-1}) approaching that for CO at the same pH. Identical k_{cat}/K_m values would indicate that at sufficiently negative redox potentials, and at concentrations well below their K_m values, CO and CO_2 are utilized at equal rates for the ACS-catalyzed formation of acetyl-CoA. That k_{cat,CO_2} obtained at these potentials (920 min^{-1}) is within error of that obtained for CO (900 min^{-1}) indicates that these alternate pathways to product may share the same RDS.

While U4AT provides the best fit with the lowest level of complexity, M4AT and U4AO cannot be excluded (refer to Table 1 for relative errors and number of unknowns for each mechanism). M4AT is identical to U4AT except that inhibitory CO molecules are assumed to bind both forms ECO and E. Simulations using M4AT fit the data as well as U4AT; however, the inhibitory binding of CO to E was so weak (4CO + E ⇌ $(CO)_4$E; the K_i values were >400 mM) that this process did not contribute noticeably to the inhibition. U4AO, shown in Figure 5B, differs from U4AT in that residual activity is assumed to arise from the partially inhibited enzyme form $(CO)_4$ECO. The best-fit simulation using U4AO fit the data as well as U4AT, but the competitive binding of CO was made so

(53) To take the heterogeneity of ACS into account, the apparent kinetic parameters reported here should be divided by 0.3−0.4. Thus, the k_{cat} values reported here, while higher than any others reported to date, may underestimate the true values by a factor of 2.5−3.3.

weak (K_i values >20 M CO) that this binding step could be ignored, and removing this step did not affect the simulation.

All other mechanisms examined either yielded poorer fits relative to U4AT or else contained substantially more unknown parameters. U1AT, U2AT, U3AT, U5AT, and U6AT are identical to U4AT except for involving 1, 2, 3, 5, or 6 inhibitory CO molecules, respectively. Simulations using U1AT and U2AT did not fit the data satisfactorily. Fits using U3AT, U5AT, and U6AT were acceptable. U6AT was excluded because the marginal improvement in fit relative to U5AT could not be justified by the additional complexity. C4AT was identical to U4AT except that CO inhibited catalysis by binding to the same enzyme form as that to which substrates CO and CO_2 bind (form E). The relative error of C4AT excluded it. R4AT was identical to U4AT except that the first inhibition step was assumed to be a reduction producing CO_2 rather than a binding event (the other three were binding steps). However, simulations using R4AT yielded a relative error high enough for it to be excluded. U4NT lacked the activation step of U4AT, and failed to fit the data at low [CO] (Figure 1 inset, dashed line), and was excluded.

Discussion

In this study, steady-state rates of acetyl-CoA synthesis were measured at various [CO] and [CO_2]. Results were analyzed by constructing various candidate kinetic models, deriving the corresponding steady-state rate equations, and then attempting to simulate the data using these equations. Comparing which model could or could not simulate the data provided insight into the actual mechanism used by ACS, especially with regard to the roles of CO and CO_2.

Our results and analysis indicate that ACS is activated for catalysis by binding CO and possibly by an associated reduction of a redox center in the enzyme. Candidate mechanisms that did not include activation failed to fit the data, especially in the region between 0 and 20 μM CO. As evident from the double-reciprocal plot in the inset of Figure 1, the activity increased more sharply than it would have in the absence of activation. Since ACS is active in the presence of CO_2 (and reductant) and in the absence of CO, we presume that CO_2 and reductant also activate the enzyme. This suggests that activation involves the binding of these molecules in conjunction with a redox process. Relative to inactivated enzyme form E′, activated enzyme E may have either CO or CO_2 bound, and/or it may be two-electrons more reduced. Activation probably does not simply involve the binding of CO or CO_2, as this would not result in the same activated state. The site of activation may be the C-cluster as it is the site of CO/CO_2 redox catalysis. Another possibility that is compatible with an earlier study[9] is that CO or CO_2/$2e^-$/$2H^+$ activate the enzyme by binding to the modulator site.

Our results and analysis also indicate that, at higher [CO], CO and the undifferentiated substrate composed of CO_2, reductant, and protons compete for the same activated enzyme form (E). While our data do not specify the CO/CO_2 binding site, it is undoubtedly the C-cluster, the active site where CO_2 is reduced to CO, as this reduction must occur before CO_2 could be used as a substrate for acetyl-CoA synthesis. Our previous study[19] suggests that CO molecules obtained by reducing CO_2 migrate to the A-cluster via a molecular tunnel. The competition observed here between CO_2 and CO molecules *not* derived from CO_2 suggests that such CO molecules also migrate to the A-cluster via the C-cluster and tunnel.

This study demonstrates that at even higher [CO], CO inhibits acetyl-CoA synthesis by binding to a different form of the

enzyme than that to which substrates bind. The inhibition is unusually sensitive to small changes in [CO], and only simulations that assumed positive cooperative binding of >2 CO's were able to mimic this sensitivity. In a potentiometric study by Russell and Lindahl[26] ACS was found to exhibit positive redox cooperativity, further evidence for the presence cooperative interactions between CO and the enzyme. That the inhibition is uncompetitive became apparent when we tried to fit models assuming mixed or competitive inhibition to the data. Moreover, if CO inhibition were competitive, the extent of inhibition would be depressed in the presence of CO_2. In fact, inhibition is not affected by CO_2 (Figure 2). The site to which these CO molecules bind is uncertain, but the A-cluster is a likely possibility, and the A_{red}-CO state of this cluster may be unable to proceed to products.[3,14,15,54] Other scenarios in which the inhibitor binds to a distinct enzyme species that arises after product release are also possible.[55]

Our results and analysis reveal that CO-inhibition is partial, and that a residual activity remains at the highest CO concentrations employed. This is the only activity that was evident from previous studies, which were performed at concentrations (980 μM, 1 atm) higher than those at which the major activity is evident.[15,50−52] We have considered two ways in which the major and residual activities may be related. The residual activity may arise from a heterogeneous form of the enzyme, and result from a catalytic mechanism distinct from the major activity. According to this view, CO would be a Michaelis−Menten substrate but not an inhibitor or an activator of the residual activity. Alternatively, the residual activity may arise from the CO-

Figure 6. Proposed mechanism by which ACS discriminates between substrate CO/CO_2 and inhibitor CO in terms of different pathways to the A-cluster. See text for details.

inhibited form of the enzyme associated with the major activity mechanism of catalysis (form $(CO)_nECO$), which may correspond to A_{red}-CO. We are unable to distinguish these possibilities.

Finally, why is CO_2 a substrate but *not* an inhibitor of the major activity while CO is *both* a substrate and inhibitor? One possibility is that at moderate [CO], CO and CO_2 bind at the C-cluster, and that the resulting CO molecules travel through the tunnel to the A-cluster where they serve as substrates in acetyl-CoA synthesis. CO likely inhibits the enzyme by binding the A-cluster, for example, by converting the diamagnetic oxidized state A_{ox} state to the A_{red}-CO state. Do these inhibitory CO molecules access the A-cluster directly from solution or from the C-cluster through the tunnel? The latter possibility appears unlikely, because once a CO molecule dissociates from the C-cluster and migrates toward the A-cluster, ACS would be unable to differentiate between CO destined to serve as a substrate and CO destined to inhibit catalysis. We propose (Figure 6) that CO molecules inhibiting catalysis bind to the A-cluster directly from solution, and do not travel to the A-cluster via the C-cluster and tunnel. In contrast, CO molecules that serve as substrate travel through the tunnel. It is fascinating to consider mechanisms that might enable ACS to distinguish between CO molecules arriving from the tunnel and those coming directly from solution. While molecular tunnels have been found in other multifunctional enzymes, this study may be the first example of an enzyme that utilizes its tunnel to discriminate between two identical molecules with diametrically opposed effects.

Supporting Information Available: Derivation of steady-state rate equations for all mechanisms (PDF). This material is available free of charge via the Internet at http://pubs.acs.org.

(54) Not all previously published results may appear compatible with this proposal. Analysis of the hyperfine splitting of the NiFeC EPR signal (from the A_{red}-CO state) as well as the corresponding ENDOR spectra of ^{13}CO-reacted ACS indicate a *single* CO bound at the A-cluster.[56] A single CO is also suggested by the IR spectra of enzyme in this state.[57] Strictly viewed, these results *are* compatible with this proposal, since our results do not require that all inhibitory CO's bind to the same site, only that they bind cooperatively. Another potential discrepancy involves the strength of CO inhibition. In an EPR/redox titration study, Russell and Lindahl estimated the K_d for CO binding to the A-cluster in the A_{red}-CO state to be ~3 and 0.3 μM in the absence and presence of CO_2, respectively,[26] while the values obtained here are substantially weaker. This apparent discrepancy may arise from differences in the way the two experiments were performed. The experiments by Russell and Lindahl were performed in the absence of the other substrates required for acetyl-CoA activity, while they were present in this study. If one of those substrates (e.g. CH_3-$Co^{3+}FeSP$) competed with the inhibitory CO's for binding to the A-cluster, the apparent K_d values measured here could underestimate true values. Further studies are required to settle this issue.

(55) Cennamo, C. *J. Theor. Biol.* **1968**, *21*, 260−277.

(56) Fan, C.; Gorst, C. M.; Ragsdale, S. W.; Hoffman, B. M. *Biochemistry* **1991**, *30*, 431−435.

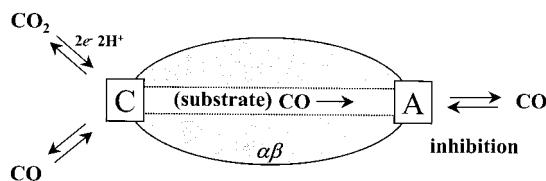(57) Kumar, M.; Ragsdale, S. W. *J. Am. Chem. Soc.* **1992**, *114*, 8713−8715.